Elman Neural Network Based on Particle Swarm Optimization for Prediction of GPS Rapid Clock Bias

Yifeng Liang, Jiangning Xu, and Miao Wu(✉)

Naval University of Engineering, Wuhan 430033, China
Wumiao9387@163.com

Abstract. To improve the accuracy of the satellite rapid clock bias, a modified Elman neural network clock bias prediction method based on particle swarm optimization (PSO) algorithm is proposed. The Elman recurrent neural network is introduced to predict the clock bias, its weights and thresholds are improved by PSO algorithm to improve the training speed and prediction accuracy. Then, the optimization method is applied to the rapid clock bias prediction, and the steps of using this method for the rapid clock bias prediction are given. Finally, the optimization method is compared with common quadratic polynomial model, gray model and ultra rapid clock bias product IGU-P. The results show that the PSO-Elman model achieves high accuracy and stability for four different types of GPS satellite clock, and its prediction accuracy and stability improved by 85%, 74%, 89% and 71%, 53%, 28% compared with QPM, GM(1,1) and IGU- P products, respectively.

Keywords: Satellite atomic clock · Clock bias prediction · Elman neural network · Particle swarm optimization

1 Introduction

The Global Navigation Satellite System (GNSS) carries out positioning through time measurement. Precision time and frequency is the basic guarantee for its normal operation and providing accurate services. Satellite atomic clock bias prediction is an important prerequisite for high-precision positioning and navigation [1]. At present, the International GNSS Service (IGS) provides GPS final precision ephemeris products with the accuracy at 75ps, but there is a lag of about two weeks, which can not meet the real-time needs of users; Broadcast ephemeris and ultra rapid clock bias products can provide real-time services, but their accuracy is about 5 ns and 3 ns respectively, so it is difficult to achieve high-precision positioning and timing.

The physical characteristic model represented by quadratic polynomial model (QPM) and its extended model, the data-driven model represented by grey system model GM (1,1) and summation autoregressive moving average model (ARIMA), and the machine learning model represented by support vector machine and limit learning machine are

C. Yang and J. Xie (Eds.): *China Satellite Navigation Conference (CSNC 2022) Proceedings*, LNEE 910, pp. 361–371, 2022.
https://doi.org/10.1007/978-981-19-2576-4_32

mainly used for clock bias prediction. Because the characteristics of satellite atomic clock are affected by periodic motion, environmental change and random factors, the traditional model has some limitations in clock bias prediction: QPM is simple and suitable for short-term prediction, but the error of long-term prediction is divergent; GM (1,1) is more suitable for small data modeling, and the exploration of historical data is limited; Arima modeling and prediction steps are cumbersome [2, 3]. For the above reasons, neural network model has been gradually applied to clock bias prediction in recent years. Wang Guocheng used radial basis function (RBF) neural network to predict GPS satellite clock bias [4]. Wang Yupu proposed a wavelet neural network (WNN) clock bias prediction model and achieved ideal accuracy [5]. However, WNN's topology is difficult to determine, and the selection of RBF sample interval is lack of theoretical basis.

In recent years, recurrent neural network (RNN) with good generalization ability has shown strong adaptability in time series data analysis. As a typical structure of RNN, compared with the traditional BP neural network structure, Elman neural network adds a receiving layer that receives the feedback signal and connects the output state of the hidden layer at the previous time. It is used as the hidden layer input together with the current time network input, so it has the characteristics of local feedback and dynamic memory [6]. However, Elman adopts the gradient descent method similar to BP neural network, which is prone to slow training speed and falling into local minima. Therefore, this paper uses particle swarm optimization (PSO) to optimize the weight and threshold of Elman neural network, establishes PSO-Elman data prediction model, and applies this method to rapid clock bias prediction. Based on the rapid clock bias data provided by IGS center, the accuracy and stability of the proposed method are compared with quadratic polynomial model, grey model and IGU-P.

2 The Common Clock Bias Prediction Model

Among the commonly used clock bias prediction models, Arima modeling is complex, which is usually used to predict the long-term parameter change of clock or the residual error of clock bias fitting; Kalman filter prediction needs sufficient clock bias data. The interference of satellite clock working environment is easy to lead to the problem of filter divergence in the prediction process. The modeling process of quadratic polynomial model and grey model is concise and suitable for rapid clock bias prediction, so they are selected as the main comparison method.

2.1 Quadratic Polynomial Model (QPM)

Generally, the time difference model of satellite atomic clock can be expressed as:

$$x(t) = x_0 + y_0 t + \frac{1}{2} d t^2 + \frac{A}{2\pi f_0} \sin(2\pi f_0 + \varphi)\Big|_0^t + \sigma_1 W_1(t) + \sigma_2 \int_0^t W_2(s) ds \quad (1)$$

Among them, x_0 represents the initial phase difference, y_0 represents the initial frequency difference, and the frequency drift d is often taken as 0 for cesium atomic clock with insignificant drift rate, which is the main trend component in the time difference. As the navigation satellite clock is affected by rotation, illumination and temperature in space, its phase change has a certain periodicity, which expressed as $\frac{A}{2\pi f_0}\sin(2\pi f_0+\varphi)\big|_0^t$, is the periodic component of phase. Two independent Wiener processes $W_1(t)$, $W_2(t)$ are used to represent dominant atomic clock noises, which is the random term part of the time difference.

Since the order of magnitude of the trend term is significantly larger than the periodic term, QPM based on phase, frequency and frequency drift parameters is used to approximately characterize the physical model of satellite atomic clock. The observation equation is:

$$L_i = a_0 + a_1(t_i - t_0) + a_2(t_i - t_0)^2 + \int_{t_0}^{t_s} f(t)dt \tag{2}$$

The corresponding error equation can be obtained as follows:

$$error = a_0 + a_1(t_i - t_0) + a_2(t_i - t_0)^2 - L \tag{3}$$

a_0, a_1, a_2 can be estimated and solved by the least square method, and then extrapolated to realize the clock bias prediction. QPM has simple modeling, clear physical meaning and good short-term prediction effect, but the long-term prediction accuracy will diverge at any time when the clock parameters change. In addition, the QPM with additional periodic term is closer to the atomic clock TDOA model in form, but because the determination of periodic term requires long data, it has general effect in short-term prediction [7].

2.2 Gery System Model (GM(1,1))

The Grey system theory was proposed by Professor Deng Julong in 1982. It is mainly used to study the uncertain system of "small data and poor information", which is more in line with the characteristics of time difference. Since the clock bias data is a single variable, the corresponding grey model is GM (1,1) model. The original measurement data can be set as:

$$x^{(0)} = \{x^{(0)}(1), x^{(0)}(2), \ldots, x^{(0)}(n)\} \tag{4}$$

The main methods of studying intrinsic grey system are accumulation and subtraction. Accumulation generation can enhance the regularity of data, improve the randomness of modeling results, and have good anti noise ability. Subtraction is mainly used for data restoration. Accumulate the original measurement data at one time to generate an accumulation sequence, which is recorded as:

$$x^{(1)} = \{x^{(1)}(1), x^{(1)}(2), \ldots, x^{(1)}(n)\} \tag{5}$$

In the formula, $x^{(1)}(k) = \sum_{i=1}^{k} x^{(0)}(i), \quad k = 1, 2, \ldots, n$ expressed the whitening equation. The background value is generated immediately adjacent to the data for the primary accumulation sequence to generate the following data:

$$z^{(1)} = \{z^{(1)}(2), z^{(1)}(3), \ldots, z^{(1)}(n)\} \tag{6}$$

where $z^{(1)}(k) = 0.5 \times (x^{(1)}(k) + x^{(1)}(k-1), k = 1, 2, \ldots, n$ according to the newly generated sequence $x^{(1)}$ and $z^{(1)}$, the differential equation and whitening differential equation are established:

$$\frac{dx^{(1)}(t)}{dt} = ax^{(1)}(t) + b \tag{7}$$

$$x^{(0)}(k) = az^{(1)}(k) + b \tag{8}$$

The solution $A = [\, a \; b \,]^T$ is fitted by the least square method, and then combined with the measured initial value. Finally, the original data can be predicted by reverse differential processing of the primary accumulation sequence:

$$x^{(0)}(k+1) = (1 - e^{-a})(x^{(0)}(1) + b/a)e^{ak} \tag{9}$$

From the above model, it can be seen that GM (1,1) mainly summarizes the system operation behavior and evolution law by mining some known information. It requires small amount of data, fast operation speed and relatively ideal medium and long-term prediction accuracy in clock bias prediction.

3 Basic Principle of PSO-Elman

3.1 Elman Neural Network

Elman neural network is composed of input layer, hidden layer, receiving layer and output layer. Its principle is explained in combination with the structural diagram shown in Fig. 1: the input data information of the input layer is transmitted to the hidden layer with linear and nonlinear excitation functions. The receiving layer remembers the output value of the neural unit at the previous moment, and its delay and memory make the output and input of the hidden layer related, Therefore, it is sensitive to historical data and finally weighted in the output layer [8].

Assuming that the network input layer nodes is r, the hidden layer and the receiving layer nodes are n, the output layer nodes is m, and the external input is $u(t-1)$, the Elman neural network structure can be expressed as:

$$x(t) = f(\omega_1 x_c(t) + \omega_2(u(t-1))) \tag{10}$$

$$x_c(t) = x(t-1) \tag{11}$$

$$y(t) = g(\omega_3 x(t)) \tag{12}$$

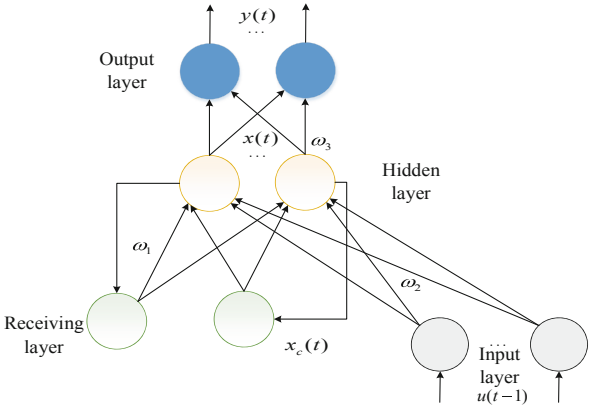

Fig. 1. Structural diagram of the Elman neural network

Among which $u(t)$ is the initial input vector, $y(t)$ is the final output vector, $x(t)$ is the node element vector of the middle layer and $x_c(t)$ is the feedback state vector. $\omega_1 \in R^{n\times n}$, $\omega_2 \in R^{n\times r}$, $\omega_3 \in R^{m\times n}$ respectively represent the connection weight matrix between the three levels. The output neuron transfer function $g(\omega_3 x(t))$ and the hidden layer neuron transfer function $f(\omega_1 x_c(t) + \omega_2(u(t-1)))$ tend to use S, such as hyperbolic tangent S and logarithmic S, and the training function is traingdx [8].

3.2 The Principle of PSO Algorithm

Particle swarm optimization algorithm was jointly proposed by Dr. Eberhart and Dr. Kennedy in 1995, whose basic core is to use the information sharing of individuals in the group to make the movement of the whole group produce an evolution process from disorder to order in the problem-solving space. PSO algorithm updates particle velocity and position by tracking individual optimal particles p_{best}^m and group optimal particles g_{best}^m during operation. The main iterative formulas are as follows:

$$v_{id}^{m+1} = \omega v_{id}^m + c_1 r_1 (p_{best}^m - x_{id}^m) + c_2 r_2 (g_{best}^m - x_{id}^m) \tag{13}$$

$$x_{id}^{m+1} = x_{id}^m + v_{id}^m \tag{14}$$

$d = 1, 2, ...K$ is the dimension of search space, $i = 1, 2, ...N$ is the population size, r_1, r_2 are random numbers between (0, 1) and c_1, c_2 are learning factors which represent the ability of particles to learn from themselves and other particles; ω is the inertia weight constant, which is used to adjust the diversity of particles; particle velocity is $v \in [v_{\min}, v_{\max}]$; m is the algebra of the current population. x_{id}^m, v_{id}^m respectively represent the current position and velocity of particles. Because there is no crossover and mutation operation process, PSO algorithm runs fast, so it is selected as the optimization method of rapid clock bias prediction.

3.3 Construction of PSO-Elman Clock Bias Prediction Model

The time series of satellite atomic clock bias is $\{x_1, x_2, ...x_N\}$, the clock bias of the past n is used to predict the clock bias of the time $n+1$, the corresponding relationship with $\{x_1, x_2, ...x_n\}$ and x_{n+1} is established, and then trained by Elman neural network. With the increase of the prediction epoch, the influence of the data farther away from the prediction epoch point on the model accuracy is gradually weakened, so the updated prediction data are continuously used for Elman neural network training.

Combined with the above flow chart, the specific steps of PSO Elman neural network clock bias prediction are introduced:

1) Because the original phase data of clock bias is not sensitive to small gross error, it is first converted into frequency data through one-time difference, then preprocessed the selected data (Set 5 times the mean square error) by using the gross error detection method based on mad, eliminated the gross error in the frequency series, interpolated the mean value, and then converted into clock bias data (Fig. 2);

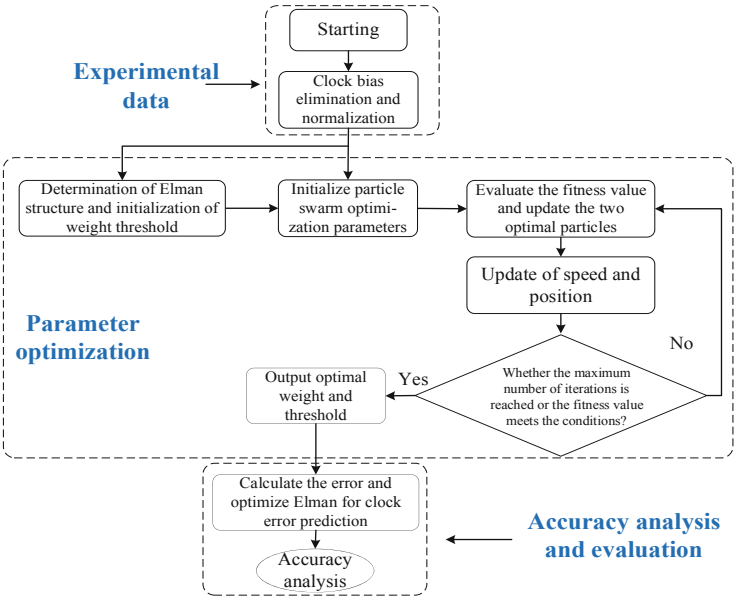

Fig. 2. Flow chart of the clock bias prediction model of the PSO-Elman neural network

2) The clock bias data set after eliminating gross errors is divided into training set and test set according to the prediction requirements, and normalized to improve the network training speed;
3) The composition of each level of Elman neural network is determined according to the number of input and output parameters, and then the particle length in PSO algorithm is determined;

4) The indirect weights and thresholds between all neurons in Elman network structure are encoded into individuals represented by real numbers, the absolute value of prediction error is taken as the individual fitness value, and the individual extreme value and global extreme value are calculated according to the fitness value;
5) Judge whether the fitness value after each iteration reaches the optimal value or whether the number of iterations reaches the maximum value. If the conditions are met, the parameter optimization process is terminated; If not, go to step 4;
6) Decode the particles corresponding to the global extreme value, take it as the initial weight and threshold of Elman network, establish the clock bias prediction model, obtain the prediction value, carry out inverse normalization processing, and analyze and evaluate the accuracy of the final output data.

4 Example Analysis

4.1 Data Sources

The precision orbit and clock bias products released by IGS center mainly include the final precision ephemeris product IGS, whose nominal accuracy is 75ps (3σ), with a delay of 12–18 days, which is generally regarded as the true value; Fast ephemeris product IGR nominal accuracy 75ps (2σ), delay 17–41 h; The observation part of the ultra rapid ephemeris product igu-o has a delay of about 3–9 h and an accuracy of 0.15 ns. The prediction part igu-p forecasts the clock bias of the day after the observation of one day, and releases it every six hours. It has strong real-time performance. However, due to the limited operation time, the accuracy is about 3ns.As of March 2, 2021, GPS on orbit satellite clock type, launch interval and corresponding number are as follows (data source: https://en.wikipedia.org/wiki/List_of_GPS_satellites) (Table 1).

Table 1. Statistical of GPS satellite atomic clock information

Type of satellite clock	Launch interval	Serial number
Block IIR Rb	1997.07–2004.11	2, 13, 16, 19, 20, 21, 22, 28
Block IIRM Rb	2005.09–2009.08	5, 7, 12, 15, 17, 29, 31
Block IIF Rb	2010.05–2016.02	1, 3, 6, 8, 9, 10, 25, 26, 27, 30, 32
Block IIF Cs	2012.10	24
Block III Rb	2018.12–2020.11	4, 18, 23, 14

Four different types of rubidium atomic clocks G02 (GPS block IIR), G05 (GPS block IIRM) and G32 (GPS block IIF) and G18 (GPS block III) with advanced design indicators are randomly selected. Among them, satellite clocks G02 and G05 have a long running time and stable working condition, and G32 and G18 are put into use later The design index is advanced and fully representative. According to the demand of GPS rapid clock bias prediction, the IGR product data of four satellite clocks for 11 days from February 20, 2021 to March 2, 2021 are taken as the test object, which are divided into

10 sections of clock bias data of two adjacent days for prediction, and the mean value is taken as the prediction accuracy index.

4.2 Experimental Verification

Experiment 1: the traditional quadratic polynomial model was used to fit the clock bias data of the first day and extrapolate the clock bias of the next day;

Experiment 2: the grey system GM (1,1) model was used to model the clock bias data of the first day and predict the clock bias of the next day;

Experiment 3: the PSO Elman clock bias prediction model established in this paper is used to train the data of the first day and predict the clock bias of the next day.

After the test is completed, the 10 prediction mean values of the corresponding accuracy (RMS) and stability (range) of the prediction duration of each satellite clock in 6 h, 12 h and 24 h of each method are statistically analyzed. In addition, the error index between igu-p products and IGR products in corresponding days will be listed as a reference for clock bias prediction accuracy. The prediction errors of different methods of the four satellite clocks are shown in Fig. 3 (a)–(d), followed by satellite clocks G02, G05, G32 and G18.The prediction accuracy and stability indexes are shown in Table 2 and 3 respectively.

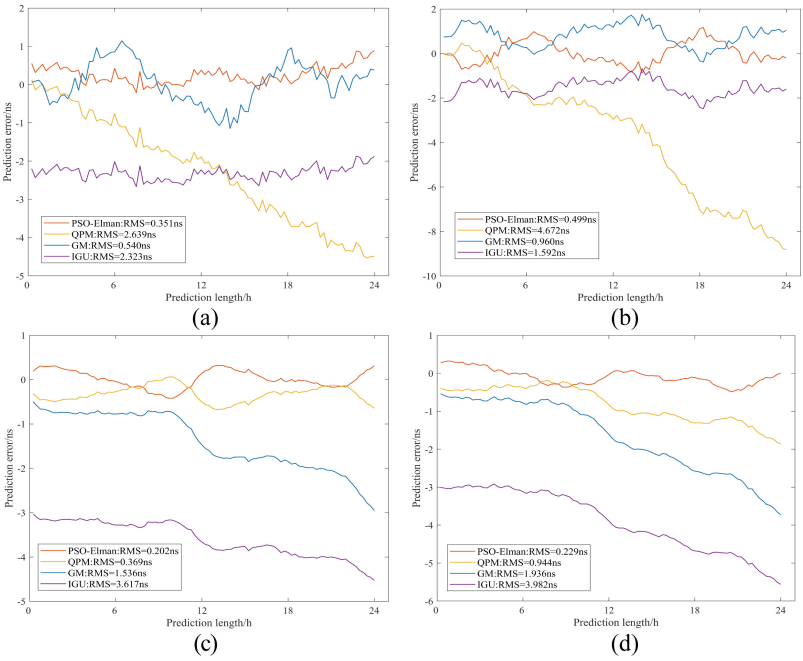

Fig. 3. The clock bias forecast error plot

The following conclusions can be drawn:

(1) The comparison of the four prediction methods shows that the prediction accuracy of the quadratic polynomial model at 6 h, 12 h and 24 h has an obvious divergence trend, and the prediction accuracy of a single day varies greatly, with a span of 0.540–4.672 ns; The variation range of grey model prediction and igu-p product error is relatively stable. The single day prediction accuracy of grey model is between 0.369–1.592 ns, and the single day error of igu-p product is between 1.936–3.982 ns. The prediction error of PSO Elman for each satellite clock is in a small range, ranging from 0.202 to 0.499 ns;

(2) The prediction errors of the four atomic clocks show that the quadratic polynomial model has large prediction errors for G02 and G05 satellite clocks with poor performance, and the prediction accuracy of single day is 2.639 ns and 4.672 ns respectively. The prediction accuracy of G32 and G18 satellite clocks with high design indexes is 0.369 ns and 0.944 ns; The grey model has slightly higher prediction accuracy for G02 and G05 atomic clocks with long operation and stable working conditions, and slightly worse prediction accuracy for G32 and G18 satellite clocks with short operation time, which is relatively stable as a whole; The igu-p product is similar to the grey model. The single day prediction accuracy of G02 and G05 satellite clocks is about 2 ns, and the prediction error of G32 and G18 satellite clocks with short operation time is close to 4 ns; The prediction accuracy of PSO Elman is positively correlated with the clock performance. Its prediction accuracy of G02 and G05 is slightly worse than G32 and G18, which can reflect the clock performance to a certain extent;

Table 2. RMS of clock bias prediction error statistics (11 day average)

Type of satellite clock		Prediction accuracy (RMS)			
		PSO-Elman	QPM	GM	IGU-P
G02 IIR Rb	6 h	0.360	0.595	0.499	2.279
	12 h	0.281	1.259	0.535	2.367
	24 h	0.351	2.639	0.540	2.323
G05 IIRM Rb	6 h	0.467	0.933	0.983	1.633
	12 h	0.468	1.783	0.953	1.563
	24 h	0.499	4.672	0.960	1.592
G32 IIF Rb	6 h	0.199	0.398	0.727	3.168
	12 h	0.231	0.315	0.818	3.237
	24 h	0.202	0.369	1.536	3.617

(*continued*)

Table 2. (*continued*)

Type of satellite clock		Prediction accuracy (RMS)			
		PSO-Elman	QPM	GM	IGU-P
G18 III Rb	6 h	0.208	0.405	0.673	3.004
	12 h	0.232	0.414	0.862	3.182
	24 h	0.229	0.944	1.936	3.982
Mean	6 h	0.309	0.583	0.721	2.521
	12 h	0.303	0.943	0.792	2.587
	24 h	0.320	2.156	1.243	2.878

(3) The average prediction accuracy of igu-p products is 2.878 ns, which is in line with the nominal accuracy of 3 ns. It can be seen from the error curve that the 6 h, 12 h and 24 h prediction error divergence trend of igu-p products is flat, but there is obvious starting point deviation, which may be caused by the difference between clock reference and IGR. Therefore, the prediction stability indexes of each method are counted. It shows that the prediction stability of igu-p products reaches 1.639 ns, which is obviously better than quadratic polynomial and grey model, but still lags behind PSO Elman model;

Table 3. Analysis of clock bias forecast stability statistics (11 day average).

Type of satellite clock	Stability of prediction(Range for 1d)			
	PSO-Elman	QPM	GM	IGU-P
G02-IIR	1.097	4.660	2.291	0.800
G05-IIRM Rb	2.055	9.293	2.138	1.797
G32-IIF	0.740	0.735	2.453	1.495
G18-III	0.809	1.682	3.186	2.463
Mean	1.175	4.093	2.517	1.639

(4) In terms of the overall prediction index, the clock bias prediction of PSO Elman model can achieve high accuracy and stability, with an average prediction accuracy of 0.320 ns, which is 85.1%, 74.2% and 88.9% higher than the commonly used quadratic polynomial prediction model, grey prediction model and igu-p products respectively; The prediction stability is 1.175 ns, which is 71.3%, 53.3% and 28.3% higher than the above three methods respectively. It shows that the prediction model better represents the nonlinear characteristics of clock bias time series, and the divergence of prediction residuals is significantly reduced.

5 Conclusion

The characteristics of existing GPS clock bias products and prediction models are introduced. Aiming at the low accuracy of rapid clock bias prediction, dynamic recursive Elman neural network is introduced into clock bias prediction. In order to further improve the speed and accuracy of clock bias prediction, the Elman neural network is optimized by PSO algorithm, and the PSO Elman clock bias prediction model is established. The results show that the average prediction accuracy of this method for 6 h, 12 h and 24 h can reach 0.309 ns, 0.303 ns and 0.320 ns respectively. Compared with the common quadratic polynomial model, grey model and igu-p product, the single day prediction accuracy is improved by 85%, 74% and 89% respectively. The error divergence trend of this method is not obvious. The average stability of single day prediction is 1.175ns, which is 71%, 53% and 28% higher than the above three methods respectively.

References

1. Zhang, X., Li, X., Guo, F., et al.: Server-based real-time precision point positioning and its application. J. Geophys. **53**(06), 1308–1314 (2010)
2. Huang, G., Wang, H., Xie, W., et al.: Technical progress of GNSS real-time satellite clock offset estimation. Navig. Positioning Timing **7**(05), 1 (2020)
3. Jiang, S., Li, B.: Application of ARIMA model in short-term satellite clock bias prediction. J. Navig. Positioning **7**(04), 118–124 (2019)
4. Wang, G., Liu, L., Xu, A., et al.: The application of radial basis function neural network in the GPS satellite clock bias prediction. Acta Geodaetica et CartographicaSinica **43**(08), 803–807+817 (2014)
5. Wang, Y., Lv, Z., Chen, H., et al.: Research on the algorithm of wavelet neural network to predict satellite clock bias. Acta Geodaetica et Cartographica Sinica **42**(03), 323–330 (2013)
6. Liu, X., Li, B., Li, J.: Application of Elman neural network model in prediction of dam deformation based on genetic algorithms. J. Water Resour. Water Eng. **25**(03), 152–156 (2014)
7. Heo, Y.J., Cho, J., Heo, M.B.: Improving prediction accuracy of GPS satellite clocks with periodic variation behavior. Meas. Sci. Technol. **21**(7), 3001–3008 (2010)
8. Mo, S., Liu, Y., Xing, H., et al.: Application of Elman neural network in neutron spectrum decomposition. J. Sichuan Univ. (Nat. Sci. Ed.) **57**(03), 531–534 (2020)